Proceedings, 7th African Rift Geothermal Conference
Kigali, Rwanda 31st October – 2nd November 2018

DIMENSIONALITY ANALYSIS OF THE OLKARIA GEOTHERMAL FIELD, EAST AFRICA RIFT

Anna W. Mwangi[13], Kevin Mickus[2] and Laura Serpa[1]

[1]University of Texas at El Paso, [2]Missouri State University, [3]Kenya Electricity Generating Company

awmwangi@miners.utep.edu

Keywords

Magnetotellurics, Geothermal, Dimensionality, Electrical strike

ABSTRACT

The Olkaria geothermal field is a Quaternary rift volcano within the central region of the Kenya rift. It is a good geothermal power producer, currently generating 687.4 MWe and has much greater potential because of recent volcanic activity. Its outline is not clearly defined but structural features such as an arc of domes intersected by prominent NNS trending faults are inferred to be the edges of a collapsed caldera. Continuous geo-scientific studies designed to understand the reservoir system are vital in expanding production.

We aim to showcase geophysical results from analyzing magnetotelluric and transient electromagnetic data from Olkaria to image the subsurface. Analyses of the dimensionality from 186 magnetotelluric stations show a NE electrical strike direction for the field. Interconnected magma plutons, located about 6-7 km below the surface as depicted by low resistivity values (5 ohm-m), control the Olkaria reservoir system. The insurgence of these magma plutons seems to be structurally controlled, upwelling along weak zones becoming the loci of a high temperature hydrothermal system.

Our findings are preliminary evidence that we can map the locations and structures of the hydrothermal system. Continued analyses of these data and other geophysical information will prove new well-defined sites where hydrothermal reservoirs can best be tapped to increase the capacity of the field.

1. Introduction

The Olkaria geothermal prospect is located among a chain of axial volcanoes aligned along the floor of the Kenyan rift valley (Figure 1). The surface geology is characterized by comenditic lava flows and pyroclastic sequences of eruption materials from itself overlain by material exuded from neighboring Mt Longonot. Recent volcanic activity within the caldera was a fissure eruption of the Olobutot fault < 200 years ago, covering the near terrain with an aa type rhyolitic lava flow. The subsurface geology in general is comprised of pyroclasts, rhyolites, trachytes, basalts and tuffs (Clarke et al., 1990; Omenda, 1998; Muchemi, 1999; Lagat, 2004).

Exploration of the field is challenging due to the complex geology and associated structures. There is no clear definition of a caldera margin and hence there is no clear understanding of the dynamics of the stress field, magma emplacement and subsequent eruption episodes. Geothermal wells sited at the production fields are very prolific for example there is a well pad site producing an average of 33 Mwe.

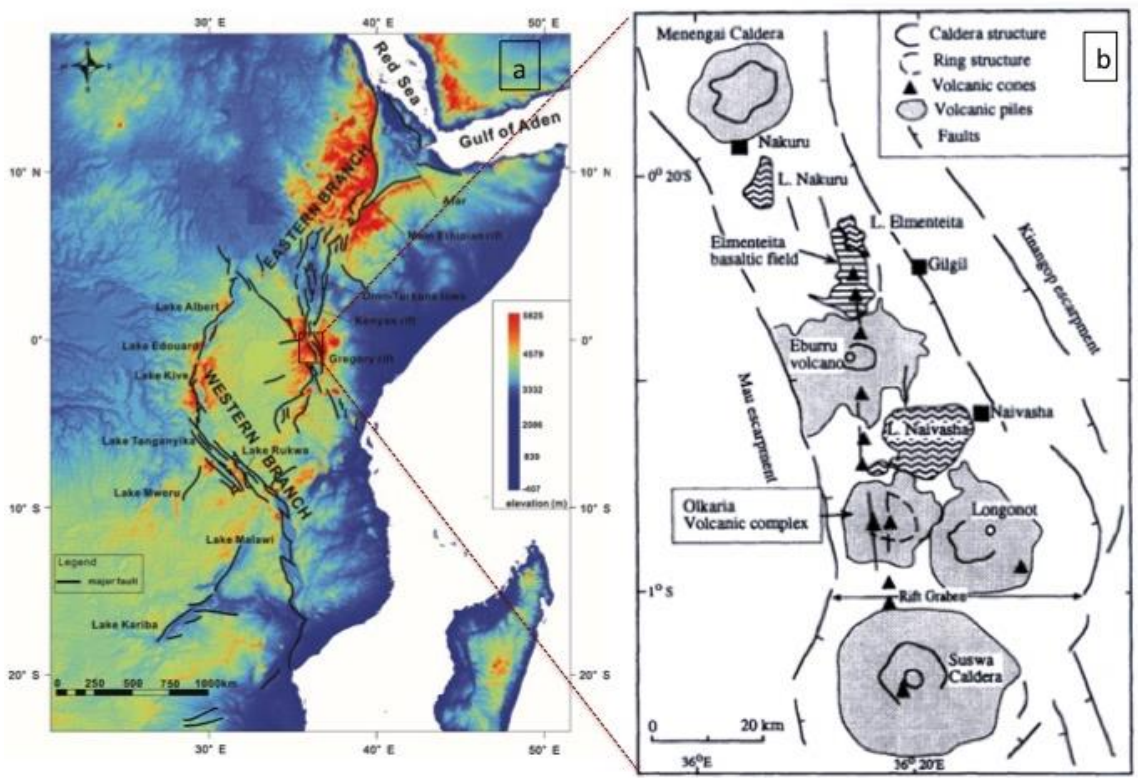

Figure 1: Location of the a) East Africa Rift system (Min and Hou, 2018) and b) central Kenya rift volcanoes including the Olkaria volcanic system (Omenda, 1998).

Geophysical studies applied to explore the geothermal field have been seismology, gravity, magnetic and electromagnetics. Active and passive seismic studies identified earthquake hypocenters around the field and suggest they originate from brittle/ductile interphase zones above the magma bodies (Simiyu, 1999; Simiyu and Keller, 2000; Simiyu and Malin, 2000). Mariita (2009) showed that magnetic minima indicate zones of demagnetization within the Olkaria caldera rocks and that these rocks have been heated above the Curie point temperature of 570^0C. Resistivity data analysis of the region east of the domes indicate a high temperature system with a low conductivity epidote-chlorite alteration zone found at 1 km below surface (Lichoro, 2009). Additionally, hydrothermal minerals such as illite, epidote

and actinolite sampled from drill cuttings from >1km depth indicate the presence of high subsurface temperature (Karingithi, 2002; Lagat, 2004; Okoo, 2013).

Thus, the purpose of this study is to define the heat sources, the structure under the caldera, associated fault systems and to zones of hot fluid up flow which can be tapped to produce more power. In order to investigate the geothermal subsurface structure of the Olkaria geothermal field, we used the electromagnetic methods of MT and transient electromagnetics (TEM). New MT and TEM data were combined with previously collected data with the aim of improving the electromagnetic imaging of the field. The analysis included determining the dimensionality, anisotropy and electrical strike direction of the MT data. These parameters will be used to create two-dimensional (2D) electrical models of the geothermal field.

2. Electromagnetic methods

Magnetotelluric methods rely on natural electromagnetic waves resulting from interaction of solar winds with earth's ionosphere and distant lightning strikes. These electromagnetic waves penetrate the earth's surface attenuating at depth where penetration depth or skin depth is dependent on the period of the wave and electrical resistivity of the subsurface material. Longer period waves will penetrate deeper into the Earth.

The central loop TEM method involves inducing an electric current along a loop into the Earth that in turn will intermittently be shut off and that decaying field induces a secondary decaying magnetic field that is measured by a receiver coil placed in the middle. From the decaying fields a voltage is induced on the receiver coil where the ground apparent resistivity values can be deduced as the eddy currents, which flow within conductors in the ground and decays characteristic of their geometry and conductance. The TEM data are used to model the near surface electrical resistivity structure and to correct the static shift problem of the MT data.

The MT data were collected as time series data and are processed in the frequency domain into electrical impedances. The electrical impedances are in a 2D Earth devolved into two perpendicular modes called the transverse magnetic (TM) and electrical (TE) modes. When the Earth is 2D, an electrical strike direction can be determined and 2D modeling can be utilized. However, most commonly the electrical structure is 3D and 2D modeling can only be used to approximate the electrical structure of a region.

To determine electrical dimensionality, the method of Martí et al. (2009) was used and to estimate the regional electrical strike direction of the data, the method of McNeice and Jones (2001) was used. The determined strike directions were then used to rotate the TM and TE data into these strike directions. The rotated TM and TE data were used to invert these data into 2D resistivity models.

2.1 Dimensionality Analysis of the Olkaria geothermal field

On average, the regional electrical strike direction for the Olkaria field is trending toward the NW-SE. This electrical strike direction is thought to be related to regional structural direction as evidenced by NW-trending faults. The NW-trending fault system may influence geothermal fluids locally where conductive ions are preferentially deposited along fluid pathways; hence their alignment will be higher within fracture zones than at the low permeable zones of the rock.

Different period bands in an MT tensor off diagonal elements often show different strike orientations and these directions depend on the dominant influencing structure at that depth. The regional electrical strike was estimated for different period bands, which show different electrical strike orientations. Thus, this will indicate dominant influencing structures at different depths. We show this by plots of the electrical strike values and the associated dimensionality of each sounding were plotted at different period bands (Figure 2). At periods between 0.1 second to 1 second, the results show some areas are 1D while there are regions that are 2D and the 3D areas are scattered. For 3D cases however there tends to be a sort of alignment. From 1 second to 100 seconds the case is majority 3D with a few cases of 2D occurring in a linear fashion (Figure 2: T=1-10 sec, T=10-100sec). The dimensionality analysis of Olkaria volcanic complex is similar to that of Menengai caldera located further north of Olkaria as shown by Wamalwa et al. (2013). Both volcanoes show a 3D structure at long periods and at short periods they show a mixture of 1D, 2D and 3D trends. Moreover, both periods show clear alignment of the electrical strike and fault orientations.

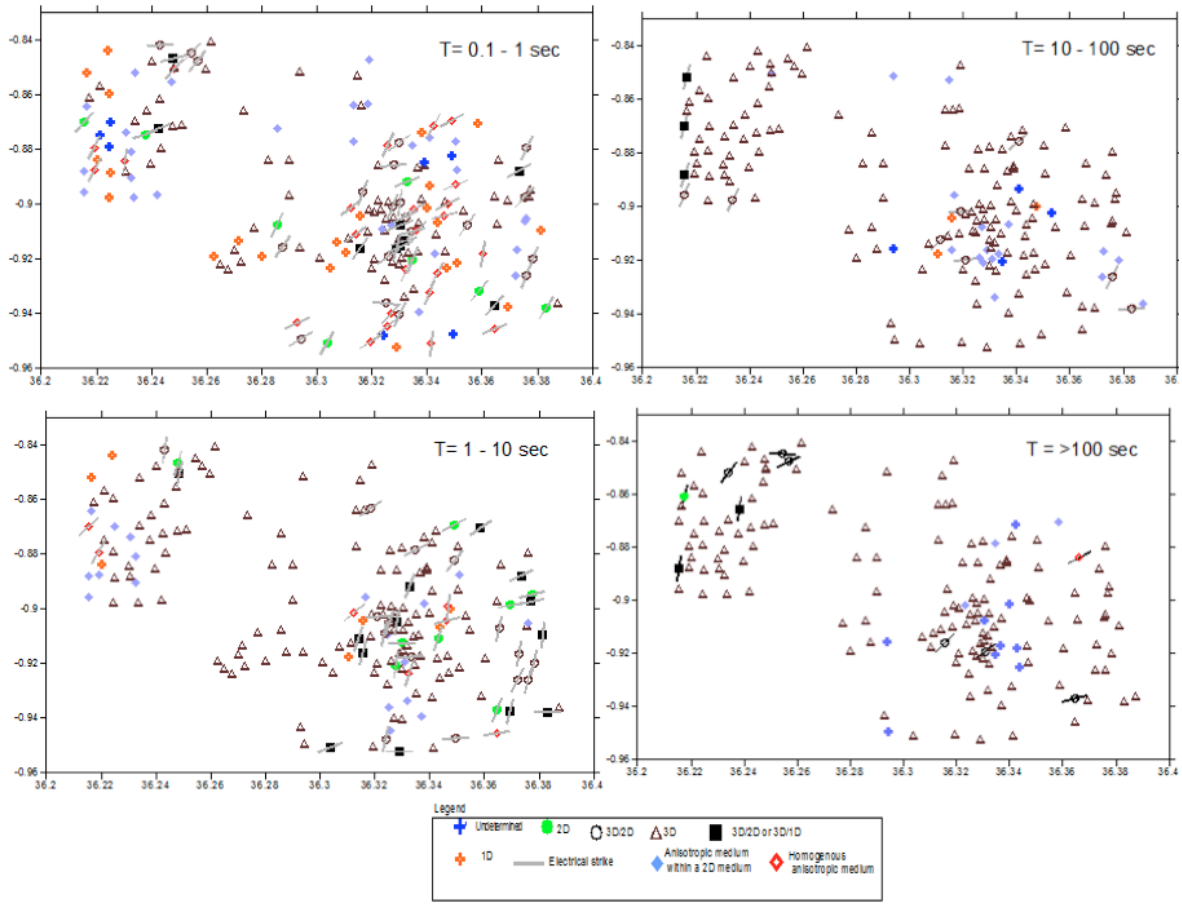

Figure 2: Dimensionality of Olkaria geothermal field, the points are MT sounding locations; various symbols show dimensionality type. The coordinate values: - latitude (x axis) and longitude (y axis) in degrees.

3. Results

The above dimensionality and regional strike analysis was used to rotate the TM and TE MT data into a preferred orientation in order to create 2D inversion models. Two profiles that cross the geothermal system were inverted. The data were static shift corrected using the TEM data, bad data were removed and the data smoothed. Figure 3 shows the location of two profiles modeled.

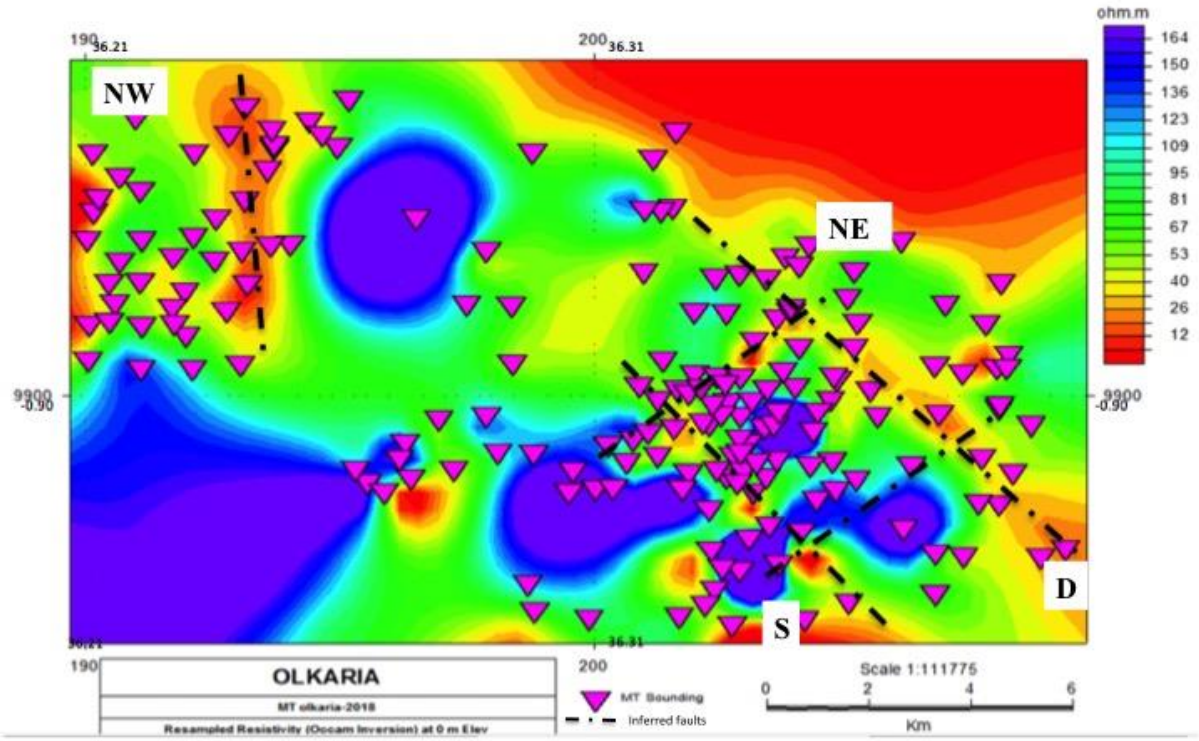

Figure 3: Resistivity slice at sea level approximately 2km depth from the surface. NW-D and S-NE profiles are the locations of two MT inverse models. The triangles are the location of MT stations. Dashed lines are faults. (UTM (km) and latitude – longitude (degrees) coordinates)

Final inverse models of profiles S-NE and NW-D are shown in Figure 4 and Figure 5 respectively. For each profile, several models were created where the inversion parameters and starting models were varied in order to create a model that was consistent with the observed data. The electrical resistivity cross sections show low resistivity at depths below 4-5 km, which we interpreted as the magma intrusion or a high heat zone, the heat source for the geothermal system.

The morphology of the heat source shows that it is interconnected with a deep magma pluton 16km deep. Upwelling of the shallow magma is along SSW direction and seems to be structurally controlled as it aligns with the inferred NE trending faults (Figure 3). Its morphology is such the shallow magma chamber is elongated along NW direction as seen in Figure 4 while Figure 5 shows its cross section in the NW direction. The shape of the low conductive cap rock indicates a doming high resistivity core coinciding with high doming elevated surface.

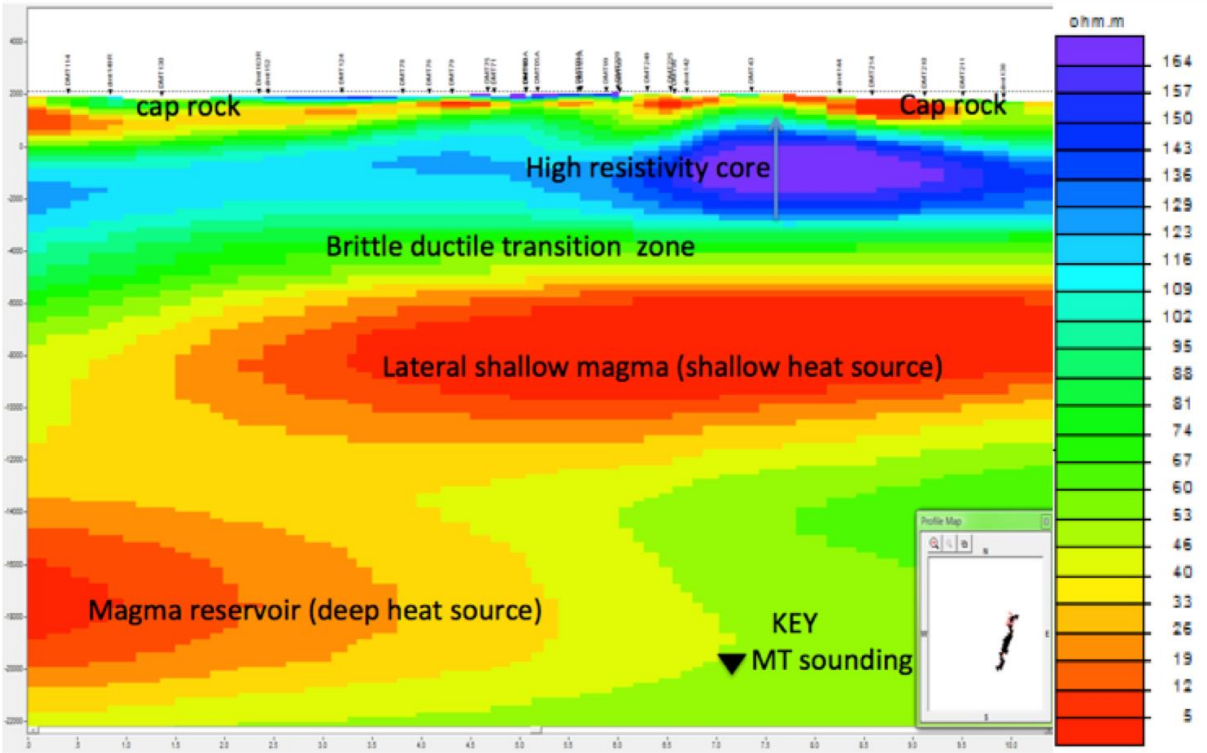

Figure 4: 2D inverse model along profile S-NE (Figure 3). The deeper high resistivity values are interpreted as high heat values above the magma chamber. The shallow magma intrusion is mapped at 6-7 km deep, the blue arrow shows peak of a doming resistivity core with doming elevation at the surface.

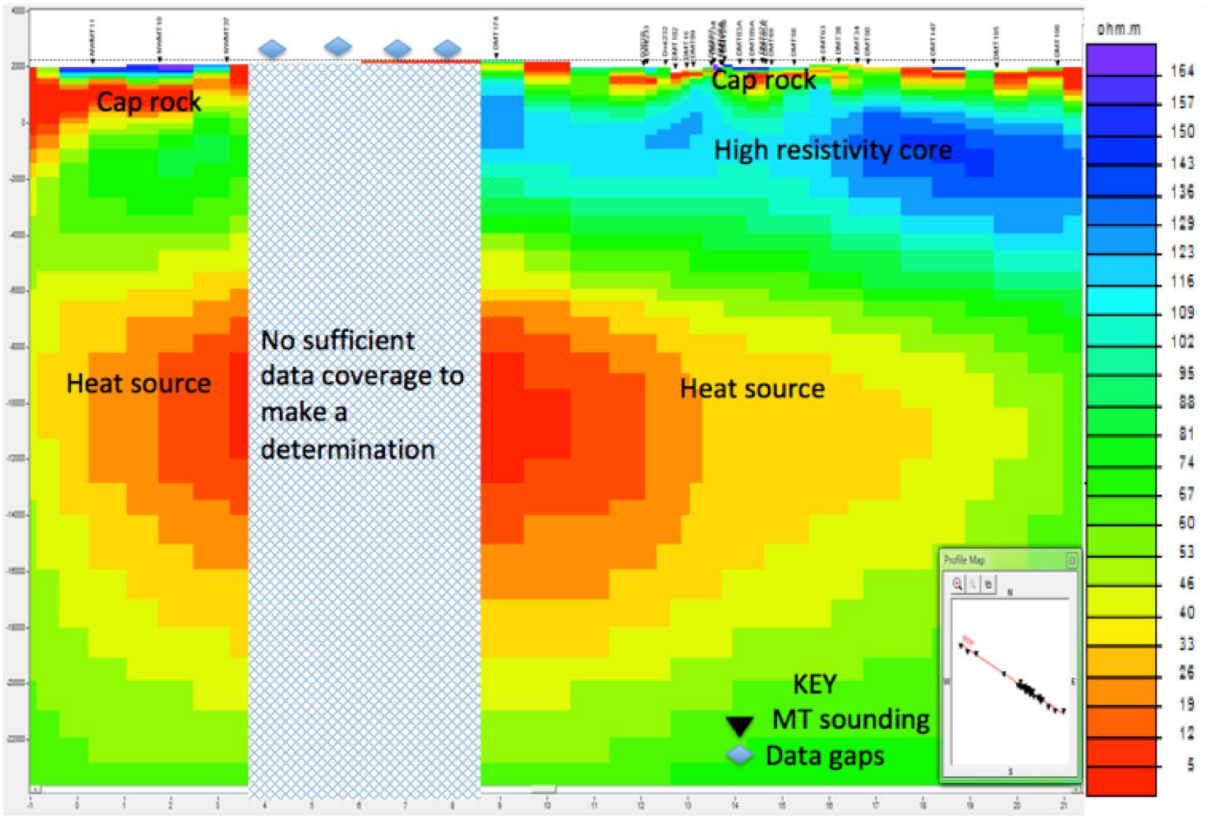

Figure 5: 2D inverse model along profile NW-D (Figure 3). The deeper low resistivity values are interpreted to be heat values above the magma chamber with an absence of the high resistivity core on the NW sector. The magma intrusion is mapped at 6-7 km deep.

4. Discussions and conclusions

A typical high resistivity core is observed directly above the heat source (55-70 ohm-m), and it is seen as a prolific reservoir zone. High temperature geothermal fields for example Krafla (Arnason and Karlsdottir, 1996) and Silali volcano (Wamalwa and Serpa, 2013; Lichoro, 2013) show a rise in resistivity in the rocks above a magma heat source. A cap rock of mixed clays (20 ohm-m) is observed overlain by a conductive smectite-zeolite minerals zone (10 ohm-m), the top of the cap rock in Figure 4 and Figure 5 and this seals the geothermal system.

The electrical resistivity response over a geothermal is distinct, because hydrothermal activity changes the host rock by dissolution or alteration of primary minerals and deposition of secondary minerals. Alteration minerals hence can be used as temperature analogues and, moreover, they have distinct resistivity signatures. Clay minerals such as smectite and zeolites have low resistivity and are formed at low temperatures.

Figure 6 indicates different alteration minerals with their associated formation temperature and resistivity values as observed in high temperature geothermal system. Electrical conduction in the unaltered rocks is determined by pore fluid present in the rocks. At low temperatures, the zeolite smectite zone and at the geothermal cap mainly comprised mixed clays minerals, electrical conductance is determined by minerals present. At deep zones where the temperature is high, chlorite and chlorite epidote zones, resistivity is influenced by pore fluid present (Arnason et al., 2000).

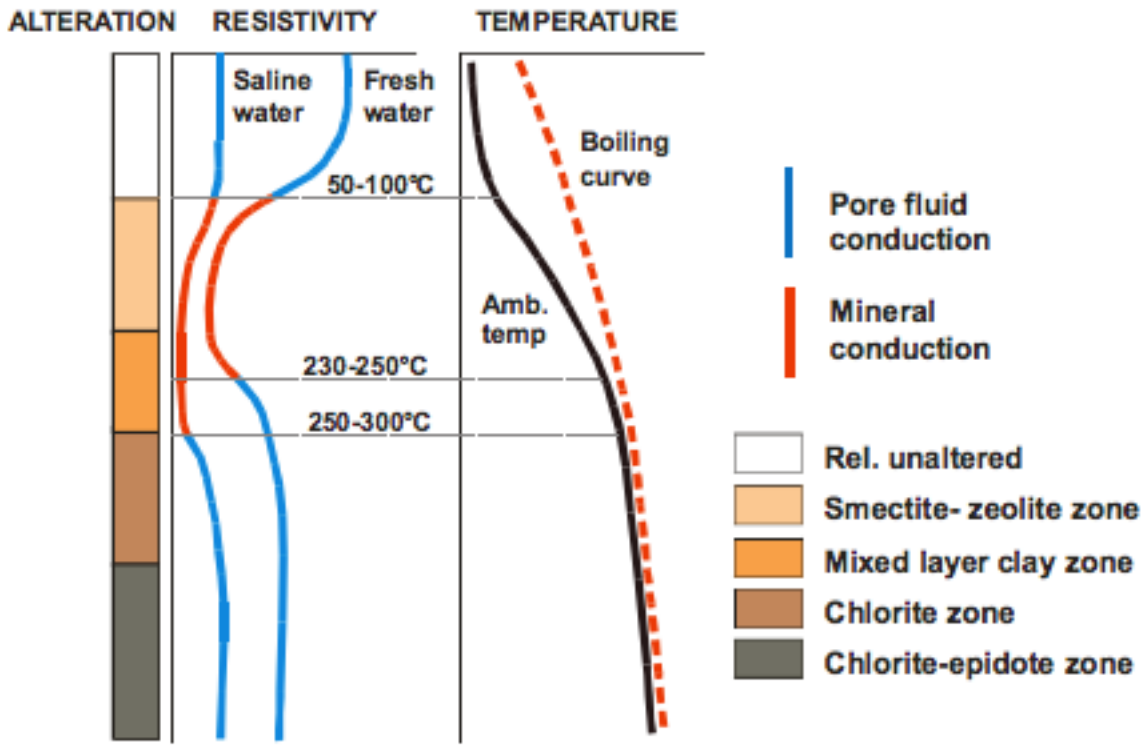

Figure 6: Generalized resistivity and temperature response over hydrothermally altered basaltic crust in Iceland (Flovenz et al., 1985).

A preliminary analysis of the MT data in the form of dimensionality, regional electrical strike directions and 2D inverse models shows that the orientation of the heat source of the geothermal system aligns with the determined electrical strike direction at deeper depths with the probability of being part of the regional structure impacting the dimensionality. 2D

inverse models show the interconnected magma chamber or high heat source at a depth of about 6 km, which roughly agrees with the deepest observed hypocentral depths of 4 km (Simiyu and Malin, 2000).

Analysis of the MT data indicates that the transition zone is located between 4-6 km depths hence, a validation of the two geophysical techniques. The geothermal system is young, well logs show high temperature indicator minerals like epidote occur at > 1 km depth and we observe from electrical resistivity models indications of high heat denoted by high resistivity core from 1.2 km depth.

Area D in Figure 4 is the domes region and the high resistivity core shows up doming, moreover, the surface is also elevated. We attribute this to a magma emplacement process and the high resistivity-high temperature zone seems to be the up flow zone (see blue arrow). We observe the low resistivity cap rock above this high temperature is dipping and getting thicker at the edges due to deposition of conductive clays. Also at depth the interconnectivity of the magma at depth in S-NE profiles mirrors the arched domes structure on the surface and we think we are roughly observing a side view part of the caldera wall. The dimensionality analysis showed the data is 3D and this is supported by the 3D nature of the underlying major structures.

This in essence shows a vibrant geothermal system in a young rift environment and our continued work will contribute to understand its volcanic evolution, definition as well as risk management in that Biggs et al. (2009) observed characteristic inflation and deflation of the Kenya rift volcanoes including Olkaria.

5. Recommendations

We recommend ways to improve electromagnetic data acquisition within the field.

- Cultural noise is prevalent in the Olkaria field stemming from the ongoing development including from electricity transmission. This results in low quality MT and TEM data near electrical installations. A speedy effort for electromagnetic data acquisition in areas with no data should be prioritized before permanent structures/activities are installed.
- To image deeper into the earth an average of 30 hours acquisition time is ideal to resolve both local and regional structures.
- Other geophysical methods such as continuous seismic data monitoring is essential to monitor volcanic activity as well constrain of electromagnetic geophysical models proposed.

REFERENCES

Arnason, K., and Karlsdottir, R., 1996, A TEM resistivity survey of the Krafla high-temperature field: OS-96005/JHD-03, 96p.

Arnason, K., Karlsdottir, R., Eysteinsson, H., Flovenz, O.G., and Gudlaugsson, S.T., 2000, The Resistivity Structure Of High-Temperature Geothermal Systems In Iceland, in Kyushu Japan, p. 6.

Biggs, J., Anthony, E.Y., and Ebinger, C.J., 2009, Multiple inflation and deflation events at Kenyan volcanoes, East African Rift: Geology, v. 37, p. 979–982.

Clarke, M.C., Woodhall, D., and Darling, G., 1990, Geological, volcanological and hydrogeological controls on the occurrence of geothermal activity in the surrounding Lake Naivasha, Kenya: British Geological Survey, 138 p.

Flovenz, O.G., Georgesson, L., and Arnason, K., 1985, Resistivity Structure of the upper crust in Iceland: v. 90-B12, p. 10,136-10,150.

Karingithi, C.W., 2002, Hydrothermal Mineral Buffers Controlling Reactive Gases Concentration In The Greater Olkaria Geothermal System, Kenya: United Nations University- Geothermal training Programme, 61 pp.

Lagat, J.K., 2004, Geology, Hydrothermal Alteration And Fluid Inclusion Studies Of Olkaria Domes Geothermal Field, Kenya: United Nations University- Geothermal training Programme, 79 pp.

Lichoro, C., 2009, Joint 1-D Inversion of TEM And MT Data from Olkaria Domes Geothermal Area, Kenya: United Nations University- Geothermal training Programme, 289–318 p.

Lichoro, C.M., 2013, Multi-Dimensional Interpretation of Electromagnetic Data From Silali Geothermal Field In Kenya: Comparison Of 1-D, 2-D and 3-D Mt Inversion: United Nations University- Geothermal training Programme, 30 pp.

Mariita, N.O., 2009, Application of Geophysics to Geothermal energy exploration and monitoring of its exploitation: Short Course IV on Exploration for Geothermal Resources, organized by. UNU-GTP, KenGen and GDC, at Lake Naivasha, Kenya (November 1-22), 9 pp.

Martí, A., Queralt, P., and Ledo, J., 2009, Waldim: A code for the dimensionality analysis of magnetotelluric data using the rotational invariants of the magnetotelluric tensor: Computers & Geosciences, v. 35, p. 2295–2303.

McNeice, G.W., and Jones, A.G., 2001, Multisite, multifrequency tensor decomposition of magnetotelluric data: Geophysics, v. 66, p. 16.

Min, G., and Hou, G., 2018, Geodynamics of the East African Rift System ∼30 Ma ago: A stress field model: Journal of Geodynamics, v. 117, p. 11 pp.

Muchemi, G., 1999, Conceptualised model of the Olkaria Geothermal Field: The Kenya Electricity Generating Company Ltd, 46 p.

Okoo, J., 2013, Borehole Geology And Hydrothermal Alteration Mineralogy Of Well Ow-39a, Olkaria Geothermal Project, Naivasha, Kenya: United Nations University-Geothermal training Programme 24, 574–576 p., http://os.is/gogn/unu-gtp-report/UNU-GTP-2013-24.pdf.

Omenda, P.A., 1998, The Geology And Structural Controls of The Olkaria Geothermal System, Kenya: Geothermics, v. 27, p. 55–74.

Simiyu, S.M., 1999, Seismic Velocity Analysis in the Olkaria Geothermal Field, in Stanford, California,v.SGP-TR-162,p.7.

Simiyu, S.M., and Keller, G.R., 2000, Seismic monitoring of the Olkaria Geothermal area, Kenya Rift valley: Journal of Volcanology and Geothermal Research, v. 95, p. 197–208.

Simiyu, S.M., and Malin, P.E., 2000, A “Volcanoseismic” Approach To Geothermal Exploration And Reservoir Monitoring: Olkaria, Kenya And Casa Diablo, Usa: Proceedings World Geothermal Congress 2000 Kyushu - Tohoku, Japan, p. 1759–1763.

Wamalwa, A.M., Mickus, K.L., and Serpa, L.F., 2013, Geophysical characterization of the Menengai volcano, Central Kenya Rift from the analysis of magnetotelluric and gravity data: Geophysics, v. 78, p. B187–B199.

Wamalwa, A.M., and Serpa, L.F., 2013, The investigation of the geothermal potential at the Silali volcano, Northern Kenya Rift, using electromagnetic data: Geothermics, v. 47, p. 89–96.